# STANDARD PROCEDURE FOR THE CALIBRATION OF DEM PARAMETERS OF COHESIONLESS BULK MATERIALS

**Andre Katterfeld and Thomas Rössler**

University of Magdeburg
Chair of Material Handling
Universitätsplatz 2, 39106 Magdeburg, Germnay
andre.katterfeld@ovgu.de

**Keywords** Calibration, Standard, Parameters, DEM, Cohesionless

**Abstract** The numerical complexity of Discrete Element Method (DEM) simulations generally forces an idealisation of DEM models, making the calibration process the key to realistic simulation results. When calibrating cohesionless, free-flowing bulk materials, individual simple experiments are commonly used as reference for the calibration, such as the angle of repose in various test methods. Regardless of the experiment, the calibration is regularly performed by trial and error, systematic variation of the parameters, or using optimisation algorithms until a suitable combination of parameters is found. A problem of the calibration, which is often ignored, is the ambiguity of these parameter combinations. Thus, there are usually a variety of contact parameters that can map the same macroscopic reference value. This paper deals in detail with the ambiguity of parameter combinations during the calibration process. It shows which standard tests can be used to generate different experimental reference values for the calibration. The results of simulations with systematic parameter variation highlight the problem of ambiguity. Subsequently it will be shown how the combination of different tests can significantly reduce the acceptable parameter combinations. A modified draw down test will be presented as a calibration test which can deliver different reference values in a single test. Hence, this calibration test allows to obtain an almost unique set of DEM parameter. The paper will show how a unique parameter setting for sliding and rolling friction can be found for cohesionless gravel with two different particle size distributions as well as the validation of the behaviour in an additional test scenario.

## 1 INTRODUCTION

The Discrete Element Method (DEM) has progressively developed into a standardised tool for the analysis of various bulk solids. Despite the steady evolution of contact models, the models continue to require a high degree of idealisation. Hence, the calibration of the DEM contact parameters is still the key factor for the successful application of replicating industrial bulk material handling systems. According to Wensrich et al. [1] the coefficients of friction (rolling and sliding) are both parameters which mainly influence the macroscopic behaviour of non-cohesive bulk materials. Common calibration experiments to determine the friction parameters for non-cohesive bulk materials include the angle of repose (AoR) test used in different variants: a lifting cylinder or funnel [1–6], a rotating drum [7–9] or after emptying a container [10–14]. In addition to these standard tests, there are a variety of other customised calibration experiments, such as the pile formation in front of a plough [15], static angles after rotation of a container [16], or avalanche-like outflow [17].

The presented calibration procedures, however, usually have a common problem. In many cases, the parameters obtained from the calibration process only consider a single calibration experiment which are not unique and hence ambiguous. The selection of a unique parameter combination is often challenging, as shown by Wensrich et al. [1], where an infinite variety of friction coefficient combinations exists for the same experimental macroscopic reference such as the AoR. Therefore, it is generally not possible to calibrate the DEM parameters with only one test result. Katterfeld [18, 19] and Derakhshani [20] showed that the independent results of several calibration tests (e.g. AoR and discharge time) can be used for finding a unique parameter set. However, they did not consider

## 2 EXPERIMENTAL INVESTIGATIONS

The obtained results of this section will be the reference values for the DEM calibration simulations and discussion sections. The calibration experiments are conducted using three kinds of tests, that all provide an AoR and a shear angle. Each of the respective experiments consider different flow regimes. These tests include: the lifting cylinder test with lifting velocity of 12 mm/s (Figure 1 a), the shear box test (Figure 1 b) and the draw down test (Figure 1 c). While the lifting cylinder test can represent a quite slow bulk material flow, the shear box test represents a high dynamical flow regime due to the rapid opening of the side wall. The draw down test is a combination of both cases and extended by a mass flow measurement.

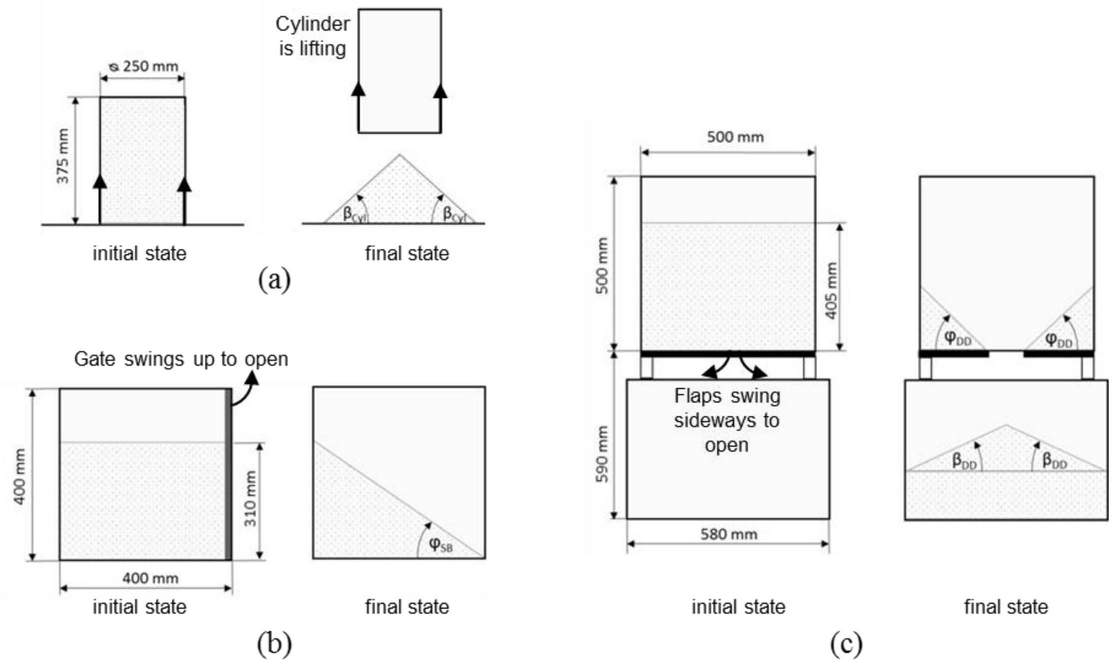


**Figure 1:** (a) Lifting cylinder test, (b) Shear box test, (c) Draw down test

For the experimental investigations, a sample of dry coarse gravel is used (Figure 2 a). It represents a typical non-cohesive, free flowing material which can be simulated using the real particle size distribution (PSD) in reasonable computing time. The corresponding PSD is given in Figure 2. The material is classified as dry, where the corresponding moisture content is 0.5% MC. The measured averaged bulk density is 1478 kg/m³. The wall friction coefficients between the bulk material sample and stainless steel and acrylic glass wall liners are determined by Jenike-wall-friction-tester [21] as

0.30 (stainless steel) and 0.36 (acrylic glass).

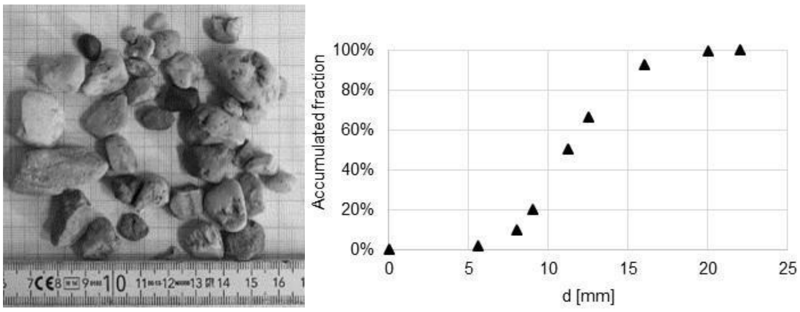


**Figure 2**: Sample of coarse gravel classified as 16/8 mm and corresponding PSD

The final state of the experiments are shown in Figure 8 in section 3. The individual reference values including mean deviations are given in Table 1. It has to be noted that difficulty arises to measure the angles with errors lower than ±1.0 deg. As the reference value of the mass flow rate, only the steady state mass flow rate is used which occurs in the time interval from 1s to 2s after initiating flow. While the measurement of the angle shows a high deviation, the mass flow rate and the measurement of the mass in the lower box have minor deviation during test repetition.

Table 1: Summary of experimental reference results

| **Experiment** | **Criteria** | **Average** | **Deviation** |
|---|---|---|---|
| | | | |
| **Cylinder** | $\beta cyl$ | 30.0 deg | ± 0.8 deg |
| | | | |
| **Shear Box** | $\varphi_{SB}$ | 35.5 deg | ± 0.7 deg |
| | | | |
| **Draw Down** | $\beta_{DD}$ | 29.8 deg | ± 1.2 deg |
| | $\varphi_{DD}$ | 38.2 deg | ± 1.1 deg |
| | $\dot{m}_{DD}$ | 10.1 kg/s | ± 0.2 kg/s |
| | $m_{DD}$ | 27.0 kg | ± 0.15 kg |

## 3 DEM CALIBRATION SIMULATIONS

### 3.1 Simulation Setup and Procedure

For the presented DEM simulations, the open source software LIGGGHTS® [22] in version 3.4.1 was used. In DEM simulations, the flow behaviour of the particles including pile formations and mass flow rates are mainly influenced by the contact parameters, particle-on-particle (sliding) friction, $\mu_s$, and rolling friction, $\mu_r$. Since spherical particles are usually used in the DEM for the simulation of real non-spherical particles, the coefficient of rolling friction must take into account the shape of the real particles [1, 3, 23]. Hence, the systematic analyses will mainly focus on the dependence of the AoR, the shear angle and the mass flow rate on the coefficients of friction.

Figure 3 shows the general flow chart that is used for the parameter study. The parameters of interest are the coefficient of sliding friction, $\mu_s$, and the coefficient of rolling friction, $\mu_r$, between the particles. These are varied systematically to span a parameter field and the resulting reference values related to the respective experiments are determined. Additionally, in case of the draw down test, the particle solid density is adjusted after filling to fit the bulk density. This is necessary, because the bulk density is the reference value given from the experiments but in the simulations the bulk density depends on the coefficient of friction. Due to the mass flow analysis in the draw down test, it is essential to match the bulk density between experiment and simulation. For the shear box test and the lifting cylinder test, this adjustment is not mandatory, because the AoR and the shear angle are not sensitive to the particle solid density [24, 25]. For the determination of the angles of repose and the shear angles, modified algorithms are used related to those published in [1, 11, 26].

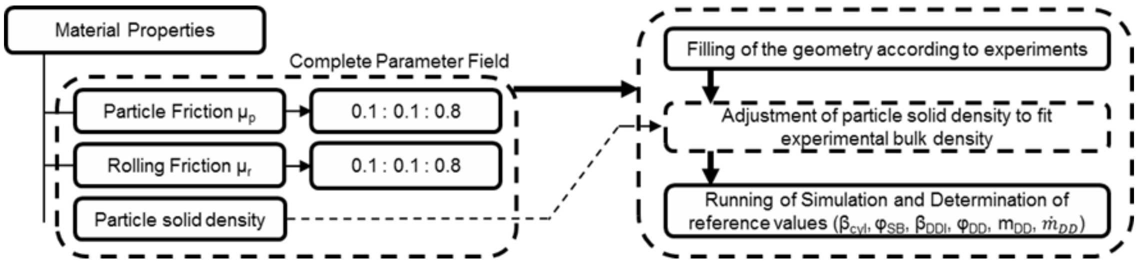


**Figure 3:** Flow chart of the calibration process

The other parameters of the DEM model are given in Table 2 and stay constant for all simulation cases. Furthermore, the particle size is not scaled or reduced and the real particle size distribution according to Figure 2 is considered at a ratio of 1:1. To reach the same filling level like in experiments, approximately 12 000, 40 000 and 32 000 particles are required for lifting cylinder test, the shear box test and the draw down test respectively.

A large number of simulations were carried out, where for each value of $\mu_s$, a range of coefficients of rolling friction, $\mu_r$, were examined. Each parameter combination was simulated twice (with different initial packing) to increase the accuracy of the results. The averaged error of AoR by using different initial packing is about ± 1.5 deg. In total 384 (3x2x64) simulations have been carried out for this series.

Table 2: General DEM parameters

| **Property** | **Unit** | **Value** |
|---|---|---|
| Contact model | - | Hertz-Mindlin (no slip) |
| Rolling friction model | - | Modified elastic plastic spring dash pot model according to Wensrich et al. [1] |
| Particle density (if not adjusted to realize the measured bulk density of 1478 kg/m³) | kg/m³ | 2463 |
| Shear modulus | Pa | 10e+7 |
| Poisson´s Ratio | - | 0.30 |
| Coefficient of restitution | - | 0.60 |
| Wall friction coefficient Gravel - Steel | - | 0.30 |
| Wall friction coefficient Gravel - Acrylic glass | - | 0.36 |
| Time step | s/step | 1.4e-5 |

### 3.2 Results of DEM Simulations

This section presents the results of the parameter study for each of the three experiments presented above. Figure 4 shows the results of the AoR of the lifting cylinder test (a) and the shear angle of the shear box test (b) as a function of the coefficient of sliding friction and rolling friction. Analogous, Figure 5 shows the results of the draw down test, namely the AoR in the lower box (a) and the shear angle (b) in the upper box. The grey coloured areas mark the experimental reference angle of each test considering a deviation interval of ± 1.5 deg. Hence, considering each experiment separately, all combinations within the grey area are able to deliver the experimental reference angle.

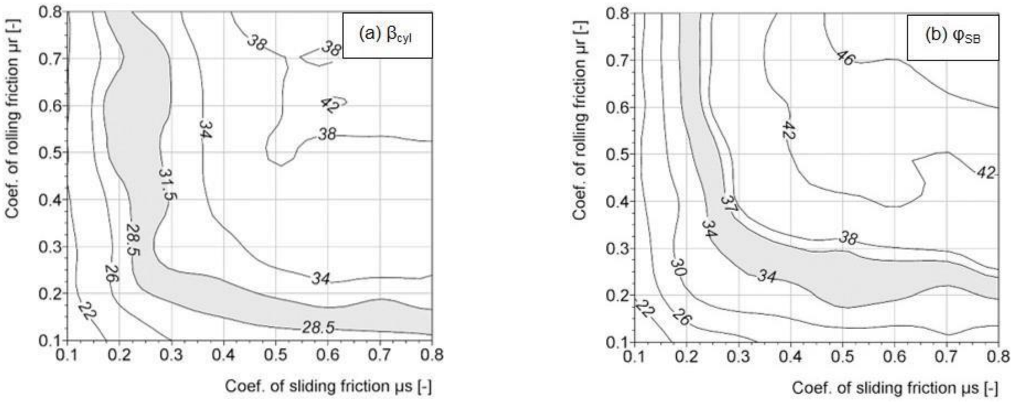


**Figure 4:** Results of (a) AoR of lifting cylinder test. (b) Shear angle of shear box test

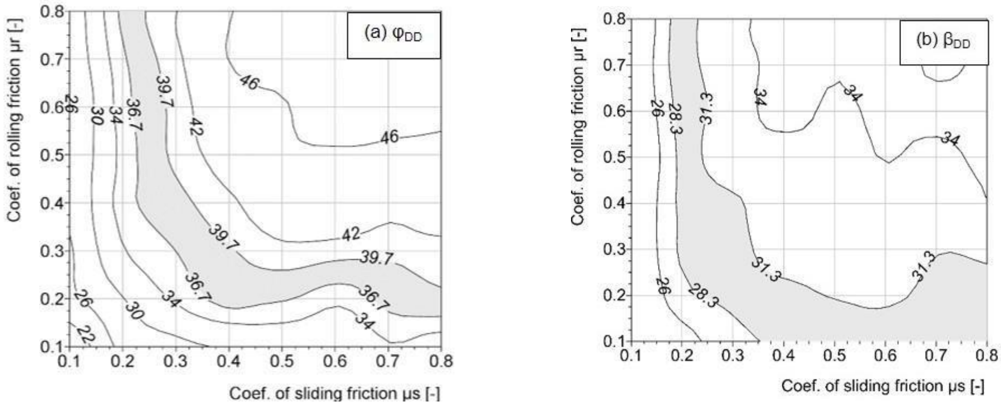


**Figure 5:** Results of Draw down test: (a) Shear Angle in the upper box. (b) AoR in the lower box.

Before the comparison and the differences are discussed in more detail, common features should be emphasised first. Regardless of the experiment, all graphs share qualitatively fundamental similarities. It can be seen that larger angles can only be achieved by increasing both values at the same time. This has been previously mentioned by Wensrich et. al. in [1]: "*The only way in which a large AoR can be achieved is if both of these mechanisms [$\mu_s$ and $\mu_r$] work together*". In contrast, it can be seen that each angle can be simulated by a multitude of combinations of both coefficients of friction. Furthermore, it can be stated that the range of permissible parameters which result in the reference value is significantly higher of the AoR result in the lower box (see Figure 5). This is generally disadvantageous for the limitation of the permissible parameter combinations. The reason for this is the change in the heap shape depending on the coefficients of friction. Hence, the determination of the AoR can be difficult in the individual case.

Two more reference criteria could be determined in the simulations of the draw down test. The discharged bulk mass in the lower box depending on the coefficient of frictions is given in Figure 6 a. The grey area highlights the area were the reference discharged mass of 27.0 kg ± 0.15 kg can be measured in the simulation. The area shape correlates qualitatively to the graphs of the different angle measurements. However, instead of higher angles, the increase in the coefficient of friction leads to a reduction of the discharged mass. The mass flow rate of the draw down test depending on the coefficients of friction is given in Figure 6 b. The grey area marks the experimental reference mass flow rate of 10.1 ± 0.3 kg/s. In contrast to the previous analysis of the shear angles and the angles of repose, the graph of the mass flow rate shows a significantly different form. The mass flow rates are greatest for small coefficients of sliding friction and decreases for increasing coefficients of sliding friction $\mu_s$. In contrast, an increase in rolling friction coefficient has minor influence on the mass flow rate. But even in this case it is not possible to distinguish which of the permissible parameter combinations is the best choice to match the experimental mass flow rate and a realistic formation of AoR. However, from the analysis of the mass flow rate it can be already concluded that the coefficient of sliding friction has to be between 0.15 and 0.25.

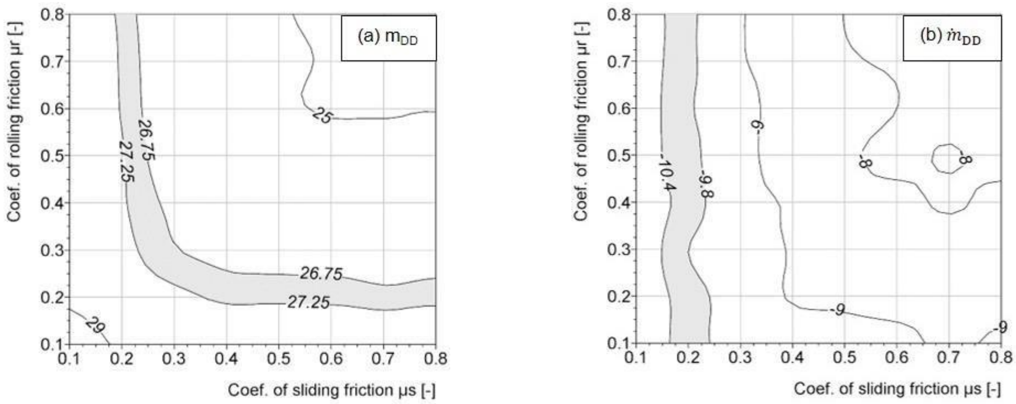


**Figure 6:** Draw down test results: (a) Discharged mass in the lower box. (b) Mass flow rate in the interval [1s; 2s].

The results above clearly show, that a single experimental value cannot be used to define a single parameter combination. However, the analysis of the mass flow rate coupled to the mass in lower box, the shear angle and the AoR can give a further improvement for the DEM calibration. In the following section the differences and problems of the single calibration experiment will discussed.

### 3.3 Comparison and Discussion of the DEM simulation results

Figure 7a shows the results of the superimposing of the shear angle, the discharged mass in the lower box and the mass flow rate of the draw down test. The black areas mark the area of superimposing, whereby all three reference criteria are fulfilled. Due to the fact that the mass flow rate is mainly sensitive to the sliding friction coefficient the permissible values of coefficient of sliding friction is further limited in comparison to just considering the shear angle and the remaining mass in the lower box. There are two areas of permissible combinations. The smaller area is in the range of $\mu_s \approx 0.23$ and $\mu_r \approx 0.425$ and the larger area is in the range of the coefficient of sliding friction between 0.18 and 0.22 and the coefficient of rolling friction values between 0.65 and 0.80. Figure 7 a clearly shows, that the rolling friction coefficient must be higher than the sliding friction coefficient. Sometimes it is argued that the value of $\mu_s$ has to be significantly higher than the one of $\mu_r$. This opinion is based on the assumption of considering spherical particles or wheels, where $\mu_r$ is approximately one percent of µs. But in the DEM simulation the spherical particles usually represent non-spherical real particles. Hence, the coefficient of rolling friction corresponds to an additional artificial rolling resistance caused by the non-sphericity and can be used as tuning parameter to represent the particle shape as described in [9]. However, the consideration of the behaviour of non-spherical particles via rolling friction is limited. Interlocking or seizing of particles can only be considered via the shape of particles.

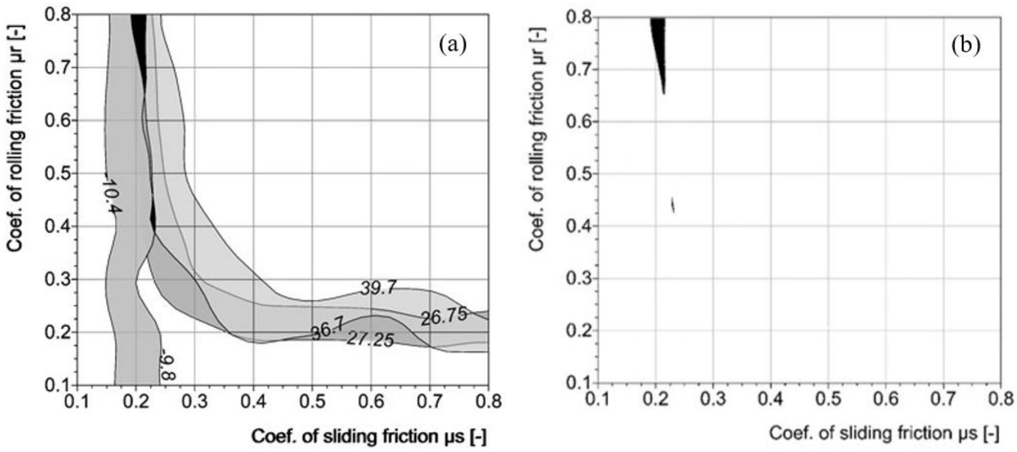


**Figure 7:** (a) Superimposing of permissible combinations of the Shear Angle, remaining mass in the lower box and the mass flow rate of the draw down test. (Black area: valid combinations to fulfil all criteria). (b) Superimposing of permissible combinations of all references

By superimposition of all tests, the valid values for the coefficient of rolling and sliding friction are slightly further limited in comparison to the results of the draw down test. For reasons of clarity, Figure 7 b only shows the area that results from superimposing all the graphs of the three individual tests (Figure 4, 5, 6). The main area stays the same like in the draw down test, while the smaller area in the range of $\mu_s \approx 0.23$ and $\mu_r \approx 0.45$ is further limited. Hence, considering the main area of permissible combinations the valid range for the coefficient of sliding friction is between 0.18 and 0.23 combined with a rolling friction coefficient between 0.65 and 0.8. The slight decrease of the valid parameter range considering the draw down test only and the draw down test plus the lifting cylinder test and shear box test shows that the draw down test alone provides a significant reduction of the valid parameter range. Hence, it might not be necessary to undertake further tests. A further refinement of the parameter / grid space is generally possible. Unfortunately, it is a very time- consuming step if a systematic parameter variation approach is used. Automated optimisation algorithms may be a better solution for the determination of a more resolved valid parameter combination.

The experiments and simulations, however, clearly show that a significant measurement error has to be taken into account especially for the measurement of angles. Hence, it must be critically questioned if the determination of DEM parameters with an accuracy of more than 1 or 2 decimal places really make sense. If values with higher accuracy are used it is very likely, that the measurement error becomes dominant and a clear distinction of the quality of the combinations is less meaningful.

### 3.4 Final Result of the DEM Calibration

The only permissible simulated combination of the grid is the one considering a coefficient of particle sliding friction of 0.2 and a rolling friction coefficient of 0.8. The adjusted particle density is 2588 kg/m³. The results of the simulation and the corresponding reference values of the experiments are given in Table 3.

Table 3: Evaluation of Calibrated Parameter Combination Results

| Test | Reference | | Experiment | Simulation | Deviation |
|---|---|---|---|---|---|
| Cylinder | AoR | $\beta_{cyl}$ | 30.0 ° | 30.6 ° | +2.0 % |
| | | | | | |
| Shear Box | Shear Angle | $\varphi_{SB}$ | 35.5 ° | 35.3 ° | -0.6 % |
| | | | | | |
| Draw Down | Shear Angle | $\varphi_{DD}$ | 38.2 ° | 37.4 ° | -2.1 % |
| | AoR | $\beta_{DD}$ | 29.8 ° | 29.9 ° | +0.3 % |
| | Mass flow rate | $\dot{m}_{DD}$ | 10.1 kg/s | 10.0 kg/s | -1.0 % |
| | Mass in box | $m_{DD}$ | 27.0 kg | 27.1 kg | +0.4 % |

The maximum deviation is 2.1 % in case of the shear angle of the draw down test. The mean deviation over all references is 1.1 %. Finally, Figure 8 shows the result of each test using the calibrated parameters $\mu_s = 0.2$ and $\mu_r = 0.8$.

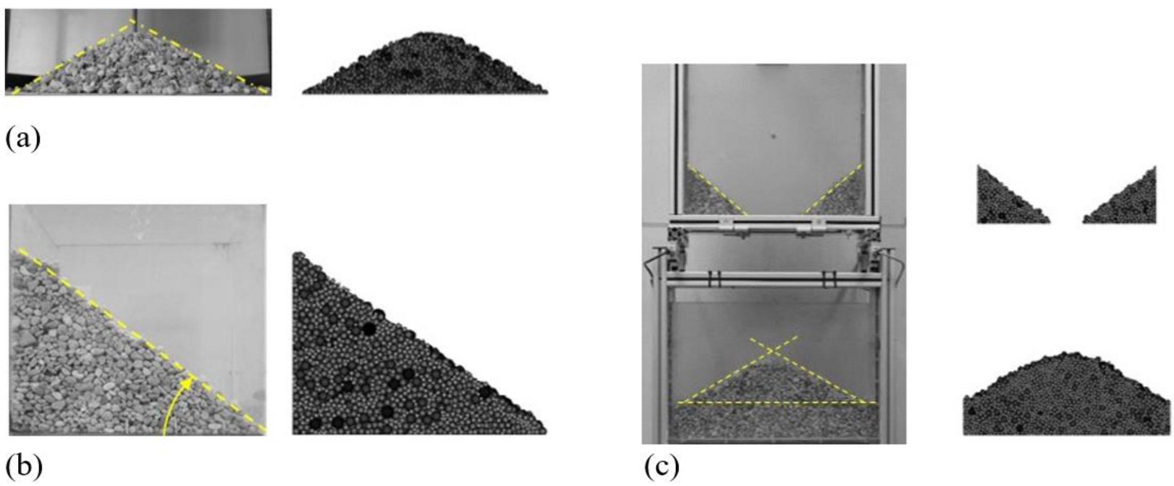


**Figure 8:** Final results of the calibration (a) lifting cylinder test, (b) shear box test, (c) draw down test

## 4 VALIDATION OF THE DETERMINED PARAMETER

To check the quality of the selected contact parameters determined in the calibration, it is essential to carry out a validation under altered flow conditions. For this purpose, first validation experiments are carried out on an annular trough test rig (Figure 9), which was developed for wear tests according to [27]. The test rig consists of a rotating annular trough with an outer diameter of 1.0 m and an inner diameter of 0.5 m, resulting in a track width of 250 mm. The trough is filled with the bulk material to a defined height of 120 mm, whereby the filling height can be adjusted by means of a vertically displaceable scraper. The scraper ensures continuous smoothing of the bulk material surface during each rotation. In the middle of the track width a plate (flat obstacle) is placed into the material stream like shown in Figure 9 (b,c). The plate is connected to a load cell, which allows the measurement of the forces acting due to the continuous material stream flow. Furthermore, the measurement of the profile of the dynamic bulk heap, which accumulates in front of the plate, is conducted by using a camera line laser triangulation. All relevant dimensions of the experimental setup are shown in Figure 9 (c).

The experiments are carried out at revolutions of 3, 6 and 9 rpm. This corresponds to flow velocities relative to the middle of the plate of 0.12, 0.24 and 0.36 m/s. The heap and force profiles are measured for 40 seconds in steady state flow condition. To perform the DEM calibration simulations, the test stand is reproduced in a simplified scale of 1:1 in the DEM, whereby only the geometries that interact with the bulk material are taken into account. Figure 9 (d) shows the test stand in the filled condition with the plate and the scraper. For the validation simulations, 5 revolutions are conducted for each revolution speed and the measurements take place in the steady state after the first revolution. The simulation parameters correspond to those from the calibration.

(a) (b) (c) (d)

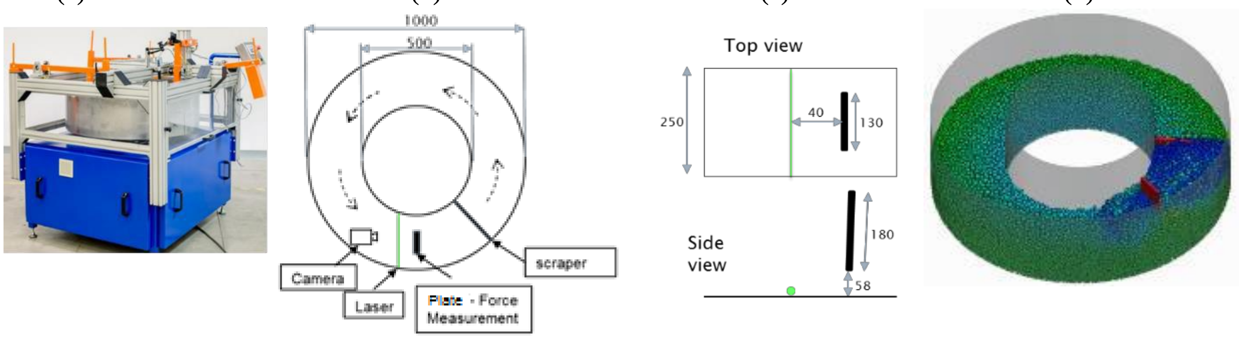


**Figure 9:** Annular trough test rig for validation (a) Build up, (b) Functioning principal in top view, (b) Positions of plate and optical laser measurement system (d) DEM simulation result

Figure 10 shows the data of the plate force measurements in the experiments and the simulations for the different rotational speeds. By taking into account the average plate forces in the steady state of both, the experiment and the simulation, Figure 11 (a) is given. The comparison shows that the forces for the different rotational speeds can be represented by using the calibrated DEM friction parameters with errors lower than 1%. Finally, Figure 11 (b) show the comparison of the heap profiles of the simulation and the experiments for 3 and 6 rpm. The red line profile represents the average experimental profile. Taking into account that it is a dynamic measurement and the experimental profiles represent only a mean value, a good agreement of both profiles can be noted.

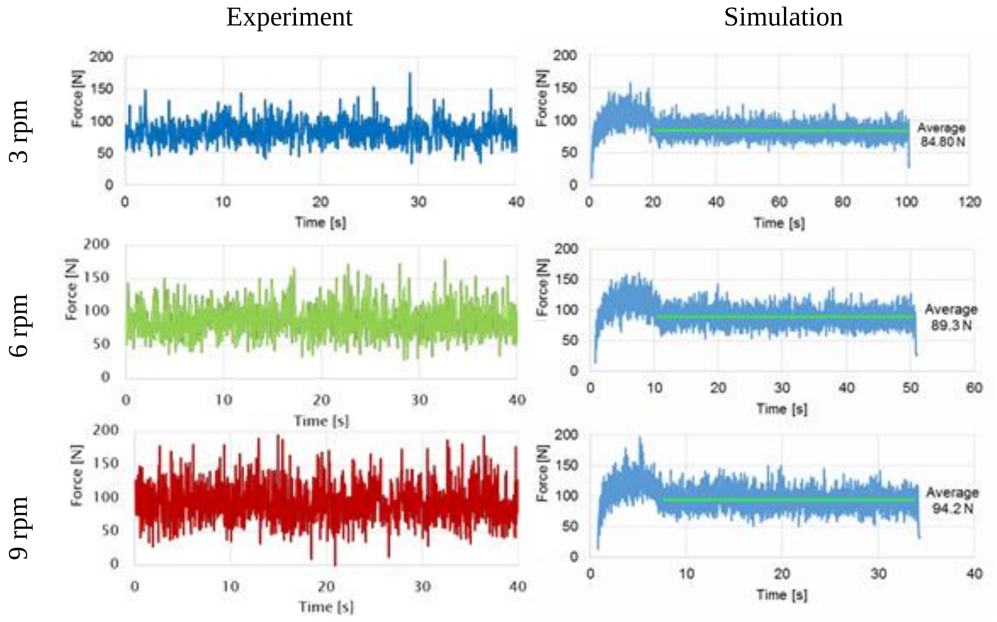


**Figure 10:** Plate force measurement in the experiment (left) and simulation (right)

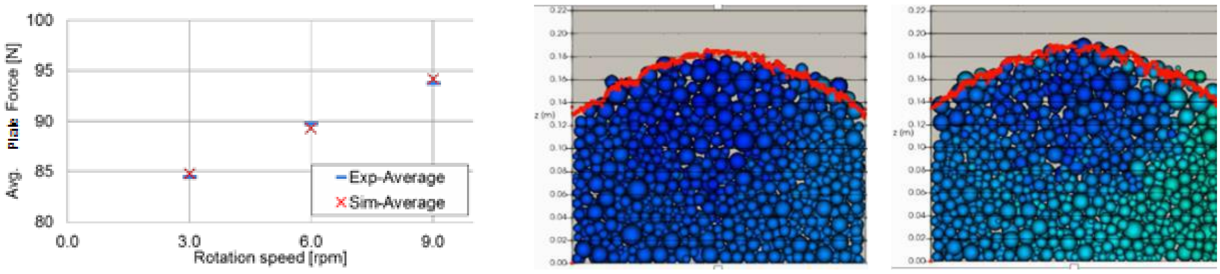


(a) (b)

**Figure 11:** Comparison between experiment and simulation: (a) average plate forces, (b) heap profiles

## 5 CONCLUSION

In the presented paper, the problem of the ambiguity of the parameter selection in the DEM calibration procedure is discussed considering different standard tests and using gravel as a non-cohesive bulk material. The different standard test rigs used in the experiments are explained in detail. Experimental reference tests and simulation series were carried out. The general dependence of the macroscopic reference criteria (AoR, shear angle, mass flow rate, and discharged mass) on the coefficients of particle sliding and rolling friction have been presented. The problem of an infinite number of friction coefficient combinations allowing to reproduce the experimental reference criteria has been shown by a systematic parameter variation. Furthermore, it was highlighted how the combination of individual tests criteria together with the consideration of measurement errors in experiment and simulation allows a clearer selection of the coefficients of friction.

Considering the effort and the quality of the permissible values, a calibration procedure using only the draw down test seems to be sufficient and accurate enough to determine a unique parameter combination. Hence, the draw down test should be used as a standard test for the calibration of DEM friction parameters for non-cohesive, free flowing bulk materials under rapid flow regimes. The presented systematic variation of the parameters has shown how the DEM calibration can be conducted using multi reference criteria from different experiments. Due to the high number of simulations and the related high computational effort, the use of a suitable optimization algorithm for a practicable application of calibration procedure is recommended. The suggested draw down test as a single test with four calibration criteria is very beneficial for an automated optimisation procedure of the DEM parameter calibration due to the reduction of numerical effort to run only one simulation model. Finally, the paper showed that calibrated DEM parameters created realistic simulation results in an independent validation experiment.

REFERENCES

[1] WENSRICH, C. M. ; KATTERFELD, A.: Rolling friction as a technique for modelling particle shape in DEM. In: Powder Technology 217 (2012), S. 409–417

[2] GRIMA, A: P: ; WYPYCH, P: W:: Discrete element simulations of granular pile formation: Method for calibrating discrete element models. In: Engineering Computations (Swansea, Wales) 28 (2011), Nr. 3, S. 314–339

[3] COETZEE, C. J.: Calibration of the discrete element method and the effect of particle shape. In: Powder Technology 297 (2016), S. 50–70

[4] LIU, F: ; ZHANG, J: ; LI, B: ; CHEN, J:: Calibration of parameters of wheat required in discrete element method simulation based on repose angle of particle heap. In: Nongye Gongcheng Xuebao/Transactions of the Chinese Society of Agricultural Engineering 32 (2016), Nr. 12, S. 247

[5] RACKL, M: ; HANLEY, K: J.: A methodical calibration procedure for discrete element models. In: Powder Technology 307 (2017), S. 73–83

[6] ADRIAN J:, FRASER, K.A.; LAIRD, G.: Improving the Precision of Discrete Element Simulations through Calibration Models. In: 13 th International LS - DYNA Users Conference, Detroit, Michigan.

[7] MARIGO, M. ; STITT, E. H.: Discrete element method (DEM) for industrial applications: Comments on calibration and validation for the modelling of cylindrical pellets. In: KONA Powder and Particle Journal (2015), Nr. 32, S. 236–252

[8] GRÖGER, T. ; KATTERFELD, A.: On the numerical calibration of discrete element models for the simulation of bulk solids. In: AIChE Annual Meeting, Conference Proceedings (2006)

[9] JUST, Sarah ; TOSCHKOFF, Gregor ; FUNKE, Adrian ; DJURIC, Dejan ; SCHARRER, Georg ; KHINAST, Johannes ; KNOP, Klaus ; KLEINEBUDDE, Peter: Experimental analysis of tablet properties for discrete element modeling of an active coating process. In: AAPS PharmSciTech 14 (2013), Nr. 1, S. 402

[10] BIERWISCH, C. S.: Numerical simulations of granular flow and filling. Zugl.: Freiburg (Breisgau), Univ., Diss., 2009. Aachen : Shaker, 2009 (Berichte aus der Physik 2009,4)

[11] CHEN, W. ; ROBERTS, A. ; KATTERFELD, A. ; WHEELER, C.: Modelling the stability of iron ore bulk cargoes during marine transport. In: Powder Technology 326 (2018), S. 255–264

[12] WEILER, R.; RIPP, M.; DAU, G.; RIPPERGER, S.: Anwendung der Diskrete- Elemente-Methode zur Simulation des Verhaltens von Schüttgütern. In: Chemie-Ingenieur-Technik 81 (2009),Nr. 6, S. 749–757

[13] ZHOU, Y. C. ; XU, B. H. ; YU, A. B. ; ZULLI, P.: An experimental and numerical study of the angle of repose of coarse spheres. In: Powder Technology 125 (2002), Nr. 1, S. 45–54

[14] GONZÁLEZ-MONTELLANO, C. ; GALLEGO, E. ; RAMÍREZ-GÓMEZ, Á ; AYUGA, F.: Three dimensional discrete element models for simulating the filling and emptying of silos:

Analysis of numerical results. In:Computers and Chemical Engineering 40 (2012), S. 22–32

[15] OTTO, H.; RICHTER, C.; KATTERFELD, A.: Validation of coupled discrete element and multi body simulations in material handling. In: CFDEM®conference : LIGGGHTS® : CFDEM®coupling : ParScale : 14.-15. September 2017, Linz, Austria : Book of abstracts (2017),

[16] CHEN, G.: Surface wear reduction of bulk solids handling equipment using bionic design. Delft, The Netherlands : TRAIL, 2017 (TRAIL thesis series, 1566-0788 T2017/8)

[17] SEN, M. ; KARKALA, S.; PANIKAR, S. ; LYNGBERG, O. ; JOHNSON, M. ; MARCHUT, A.; SCHÄFER, E. ; RAMACHANDRAN, R.: Analyzing the Mixing Dynamics of an Industrial Batch Bin Blender via Discrete Element Modeling Method. In: Processes 5 (2017), Nr. 4, S. 22

[18] KATTERFELD, A. ; DONOHUE, T. J. ; ILIC, D.: Application of the discrete element method in mechanical conveying of bulk materials. In: 7th International Conference for Conveying and Handling of Particulate Solids (CHoPS) : 10.09.2012 - 13.09.2012, Friedrichshafen/Germany (2012)

[19] KATTERFELD, A.; DONOHUE, T. ; ILIC, D. ; WENSRICH, C.: On the calibration of DEM parameters for the simulation of bulk materials under dynamic conditions. In: ICBMH 2013 : 11th International Conference on Bulk Materials Storage, Handling & Transportation ; 2 - 4 July 2013, Newcastle, Australia (2013)

[20] DERAKHSHANI, S. M.: Modelling dust liberation in bulk material handling systems. PhD Thesis. TU Delft, The Netherlands, 2016

[21] JENIKE, A. W.: Storage and flow of solids. 13. print. Salt Lake City, Utah : Univ. of Utah, 1989 (Bulletin / Utah Engineering Experiment Station 123)

[22] KLOSS, C.; GONIVA, C.; HAGER, A.; AMBERGER, S. ; PIRKER, S.: Models, algorithms and validation for opensource DEM and CFD-DEM. In: Progress in Computational Fluid Dynamics 12 (2012), 2-3, S. 140–152

[23] CLEARY, P. W. ; SAWLEY, M. L.: DEM modelling of industrial granular flows: 3D case studies and the effect of particle shape on hopper discharge. In: Applied Mathematical Modelling 26 (2002), Nr. 2, S. 89– 111

[24] ZHOU, Y. C. ; XU, B. H. ; YU, A. B. ; ZULLI, P.: Numerical investigation of the angle of repose of monosized spheres. In: Physical review. E, Statistical, nonlinear, and soft matter physics 64 (2001), 2 Pt 1, S. 21301

[25] DERAKHSHANI, S. M. ; SCHOTT, D. L. ; LODEWIJKS, G.: Reducing computation time of dem simulations of fine granular materials. In: Bulk Solids Handling 33 (2013), Nr. 6, S. 52

[26] ROESSLER, T. ; KATTERFELD, A.: Scaling of the angle of repose test and its influence on the calibration of DEM parameters using upscaled particles. In: Powder Technology 330 (2018),

[27] WICHE, S.J.; KEYS, S.; ROBERTS, A.W.: Abrasion wear tester for bulk solids handling application. In: Wear, Volume 258, Issues 1–4, 2005